

Incident-polarization-independent spin Hall effect of light reaching a half beam waist

Minkyung Kim¹, Dasol Lee², and Junsuk Rho^{1,3,4,*}

¹Department of Mechanical Engineering, Pohang University of Science and Technology (POSTECH), Pohang 37673, Republic of Korea

²Department of Biomedical Engineering, Yonsei University, Wonju 26493, Republic of Korea

³Department of Chemical Engineering, Pohang University of Science and Technology (POSTECH), Pohang 37673, Republic of Korea

⁴POSCO-POSTECH-RIST Convergence Research Center for Flat Optics and Metaphotonics, Pohang 37673, Republic of Korea

*jsrho@postech.ac.kr

Abstract

The spin Hall effect of light, a spin-dependent transverse splitting of light at an optical interface, is intrinsically an incident-polarization-sensitive phenomenon. Recently, an approach to eliminate the polarization dependence by equalizing the reflection coefficients of two linear polarizations has been proposed, but is only valid when the beam waist is sufficiently larger than the wavelength. Here, we demonstrate that an interface, at which the reflection coefficients of the two linear polarizations are the same and so are their derivatives with respect to the incident angle, supports the polarization-independent spin Hall shift, even when the beam waist is comparable to the wavelength. In addition, an isotropic-anisotropic interface that exhibits the polarization-independent spin Hall shift over the entire range of incident angles is presented. Monte-Carlo simulations prove that spin Hall shifts are degenerate under any polarization and reaches a half of beam waist under unpolarized incidence. We suggest an application of the beam-waist-scale spin Hall effect of light as a tunable beam-splitting device that is responsive to the incident polarization. The spin Hall shift that is independent of the incident polarization at any incident angle will facilitate a wide range of applications including practical spin-dependent devices and active beam splitters.

1 Introduction

The spin Hall effect of light (SHEL) [1–5], a spin-dependent microscopic splitting of refracted/reflected light along the transverse direction, is an optical analog of the transverse spin accumulation of electric current, called the spin Hall effect [6, 7]. A linearly polarized incidence is split into left circularly polarized light (LCP) and right circularly polarized light (RCP) that are displaced in opposite directions. The origin of the SHEL lies on a finite beam waist of the incidence that contains wave vectors with slightly different orientations and on the transversality of light [2, 8, 9], which enforces orthogonal locking between the polarization state and momentum. Wave vectors that have nonzero components along the transverse direction yield local rotations of the polarization basis, resulting in a spin-dependent position correction term in the refracted/reflected beam, perpendicular to the incident plane. Therefore, the SHEL is inherently dependent on incident polarization.

It has been reported recently that an interface that has the same reflection coefficients, i.e., $r_s = r_p$, where subscripts s and p denote incident polarization states, supports the incident-polarization-independent SHEL for the reflected beam, or equivalently transmission coefficients $t_s = -t_p$ for the refracted beam [10]. The spin Hall shifts at such an interface are degenerate under incidences that have any polarization state (Fig. 1a, b). One assumption that underlies the theoretical demonstration is that the beam waist w_0 is

much larger than wavelength λ , satisfying

$$w_0^2 \gg \left(\frac{\lambda \cot \theta_i}{2\pi} \right)^2, \quad (1)$$

where θ_i is the incident angle of the beam. We refer to this condition as a large beam waist condition hereafter for convenience. While this condition is valid in most instances except for tightly-confined or near-normal incidence, the spin Hall shift under the condition is essentially much smaller than w_0 (Fig. 1c) and breaking of the condition provides a route to increase the spin Hall shift substantially even up to $w_0/2$. Given that tremendous efforts have been devoted during the past decade to increasing the spin Hall shift from the deep-subwavelength scale to several wavelengths and even beyond [11–24], an approach to achieve polarization-independent SHEL that is valid even when w_0^2 is comparable to or less than $(\lambda \cot \theta_i / 2\pi)^2$ is in high demand (Fig. 1d).

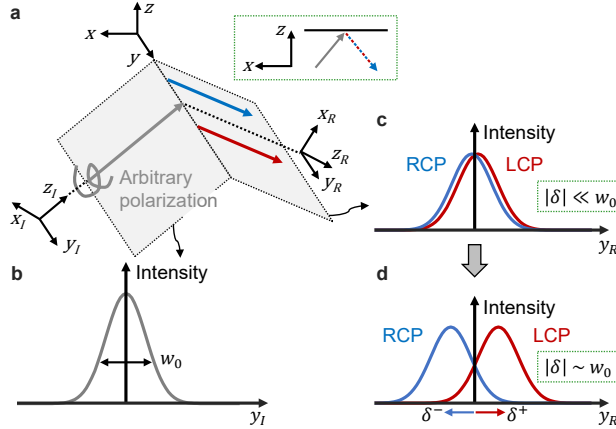


Figure 1: Schematic of the polarization-independent SHEL. (a) The SHEL of a reflected beam at an interface ($z = 0$). Inset shows a two-dimensional view in the incident plane. (b) Intensity profile of the incidence along the transverse direction. (c, d) Intensity profiles of the circularly polarized components of the reflected beam along the transverse direction when the spin Hall shift (δ) is (c) much smaller than or (d) comparable to the beam waist.

In this article, we demonstrate a gigantic SHEL that reaches $w_0/2$ and is insensitive to the incident polarization at an interface between isotropic and anisotropic media. The dependence of the spin Hall shift on incident polarization is removed even for light that does not satisfy the large beam waist condition (Eq. 1) if the Fresnel coefficients of two linear polarizations as well as their angular derivatives are equal to each other. Starting from the theoretical description to prove the polarization independence under such conditions, we demonstrate both analytically and numerically that such conditions are satisfied in the entire range of $0 < \theta_i < \pi$ if anisotropic and isotropic media adjacent to each other have permittivities that follow a certain relation. Furthermore, Monte-Carlo simulations are conducted to confirm the degenerate SHEL under arbitrarily polarized incidence. The spatial distributions of the reflected beam clearly manifest a distinguishable splitting that reaches $w_0/2$ under unpolarized incidence. This gigantic SHEL that is insensitive to the incident polarization at any θ_i opens a path towards realization of spin-sensitive and compact devices that are robust against change of incident polarization and dynamic beam splitters that operate in response to the incident polarization.

2 Conditions for the polarization-independent SHEL

This section revisits the derivation of the reflected beam profile and the spin Hall shift using a wave packet model and deduces the required conditions for polarization-independent SHEL that do not require any assumption or condition (Eq. 1). In a macroscopic view, the refraction and reflection at a planar interface are described by Snell's law and Fresnel equations. However, those equations assume a single wave vector

for each incident, refracted, and reflected beam and thus are not correct microscopically if the beams have a finite beam waist. More specifically, an incidence not only has the central wave vector parallel to the k_{Iz} -axis, but also contains noncentral wave vectors that have nonzero k_{Ix} and k_{Iy} components (Fig. 1a). Thus, two correction terms should be added, one for k_{Ix} and the other for k_{Iy} . First, to consider nonzero k_{Iy} , the Jones matrix at the interface has off-diagonal terms [11]

$$\begin{pmatrix} \psi_R^H \\ \psi_R^V \end{pmatrix} = \begin{pmatrix} r_p & \frac{k_y}{k_0}(r_p + r_s) \cot \theta_i \\ -\frac{k_y}{k_0}(r_p + r_s) \cot \theta_i & r_s \end{pmatrix} \begin{pmatrix} \psi_I^H \\ \psi_I^V \end{pmatrix}, \quad (2)$$

where superscripts H and V denote horizontal and vertical polarizations respectively, subscripts I and R correspond to the incident and reflected beam respectively, k_0 is the incident wave vector, $k_x \equiv k_{Ix} = -k_{Rx}$ and $k_y \equiv k_{Iy} = k_{Ry}$ are x - and y -components of the wave vector, and the incident and reflected beams have a Gaussian beam shape as

$$\psi_{I,R} = \begin{pmatrix} \psi_{I,R}^H \\ \psi_{I,R}^V \end{pmatrix} \frac{w_0}{\sqrt{2\pi}} \exp\left(-\frac{w_0(k_x^2 + k_y^2)}{4}\right). \quad (3)$$

Then, the nonzero k_{Ix} is considered by applying a Taylor series expansion to r_s and r_p in Eq. 2 as

$$r_{s,p} = r_{s,p}(k_{Ix} = 0) + \left. \frac{\partial r_{s,p}}{\partial k_{Ix}} \right|_{k_{Ix}=0} k_{Ix}. \quad (4)$$

Combining Eqs. 2 to 4 and applying basis transformation from linear to circular and an inverse Fourier transform provide the spatial field profiles of circularly polarized components of the reflected beam as linear equations $\tilde{\psi}_R^\pm = \tilde{\psi}_{R,H}^\pm \psi_I^H \pm i \tilde{\psi}_{R,V}^\pm \psi_I^V$ where

$$\begin{aligned} \tilde{\psi}_{R,H}^\pm &= \frac{1}{\sqrt{2\pi}w_0} \frac{z_0}{z_0 + iz_R} \exp\left(-\frac{k_0}{2} \frac{x_R^2 + y_R^2}{z_0 + iz_R}\right) \\ &\quad \times \left[r_p - i \frac{x_R}{z_0 + iz_R} \dot{r}_p \mp \frac{y_R \cot \theta_i}{z_0 + iz_R} (r_p + r_s) \mp i \frac{x_R y_R \cot \theta_i}{(z_0 + iz_R)^2} (\dot{r}_p + \dot{r}_s) \right] \exp(ik_r z_R), \\ \tilde{\psi}_{R,V}^\pm &= \frac{1}{\sqrt{2\pi}w_0} \frac{z_0}{z_0 + iz_R} \exp\left(-\frac{k_0}{2} \frac{x_R^2 + y_R^2}{z_0 + iz_R}\right) \\ &\quad \times \left[r_s - i \frac{x_R}{z_0 + iz_R} \dot{r}_s \mp \frac{y_R \cot \theta_i}{z_0 + iz_R} (r_p + r_s) \mp i \frac{x_R y_R \cot \theta_i}{(z_0 + iz_R)^2} (\dot{r}_p + \dot{r}_s) \right] \exp(ik_r z_R), \end{aligned} \quad (5)$$

where the second subscript of $\tilde{\psi}$ indicates incident polarization, the dot notation represents the derivative with respect to θ_i ($\dot{r}_{s,p} = \partial r_{s,p} / \partial \theta_i$), and $z_0 = k_0 w_0^2 / 2$ is the Rayleigh length. Taking the y position average

$$\delta^\pm = \frac{\langle \tilde{\psi}_R^\pm | y_R | \tilde{\psi}_R^\pm \rangle}{\langle \tilde{\psi}_R^\pm | \tilde{\psi}_R^\pm \rangle} \quad (6)$$

of the reflected beam provides the exact formula of the spin Hall shift [25]:

$$\begin{aligned} \delta_H^\pm &= \mp \frac{\cot \theta_i}{k_0} \frac{|r_p|^2 + \text{Re}(r_p r_s^*)}{|r_p|^2 + (\frac{\cot \theta_i}{k_0 w_0})^2 |r_p + r_s|^2 + \frac{1}{k_0^2 w_0^2} \dot{r}_p \dot{r}_p^*}, \\ \delta_V^\pm &= \mp \frac{\cot \theta_i}{k_0} \frac{|r_s|^2 + \text{Re}(r_p^* r_s)}{|r_s|^2 + (\frac{\cot \theta_i}{k_0 w_0})^2 |r_p + r_s|^2 + \frac{1}{k_0^2 w_0^2} \dot{r}_s \dot{r}_s^*}, \end{aligned} \quad (7)$$

where $*$ corresponds to the complex conjugate. Eq. 7 can be further simplified to

$$\begin{aligned} \delta_H^\pm &= \mp \frac{\cot \theta_i}{k_0} \text{Re}\left(1 + \frac{r_s}{r_p}\right), \\ \delta_V^\pm &= \mp \frac{\cot \theta_i}{k_0} \text{Re}\left(1 + \frac{r_p}{r_s}\right), \end{aligned} \quad (8)$$

under the large beam waist condition (Eq. 1).

A close examination of Eq. 5 shows that the two field profiles appear symmetrical ($r_s \rightarrow r_p$, $r_p \rightarrow r_s$, $\dot{r}_s \rightarrow \dot{r}_p$, and $\dot{r}_p \rightarrow \dot{r}_s$). Therefore, if $r_s = r_p$ and $\dot{r}_s = \dot{r}_p$, then $\tilde{\psi}_{R,H}^\pm = \tilde{\psi}_{R,V}^\pm \equiv \tilde{\psi}_{R0}^\pm$ and thus the components of the incident Jones vector ψ_I^H and ψ_I^V act only as constant coefficients of the field profile as $\tilde{\psi}_R^\pm = (\psi_I^H \pm i\psi_I^V)\tilde{\psi}_{R0}^\pm$. Then substitution of this equation to Eq. 6 provides $\delta^\pm = \langle \tilde{\psi}_{R0}^\pm | y_R | \tilde{\psi}_{R0}^\pm \rangle / \langle \tilde{\psi}_{R0}^\pm | \tilde{\psi}_{R0}^\pm \rangle$, which contains neither ψ_I^H nor ψ_I^V . Therefore, the spin Hall shift is independent of the polarization state of the incidence. Similarly, the polarization-independent SHEL can be also demonstrated for the transmitted beam if $t_s = -t_p$ and $\dot{t}_s = -\dot{t}_p$.

Importantly, although the previous condition of $r_s = r_p$ is obtained under the assumption that the wave vector deflections are much smaller than the wave number ($k_{x,y} \ll k_0$) and is valid under the large beam waist condition (Eq. 1) [10], the theoretical proof here does not rely on any assumption. Thus, the SHEL at an interface that supports $r_s = r_p$ and $\dot{r}_s = \dot{r}_p$ appears independent of the incident polarization, under any condition, even when w_0 is comparable to λ or θ_i is so small that Eq. 1 is invalid.

3 Anisotropic medium satisfying $r_s = r_p$ and $\dot{r}_s = \dot{r}_p$

This section demonstrates that an interface between isotropic and anisotropic media with a specific condition supports $r_s = r_p$ and $\dot{r}_s = \dot{r}_p$ at any θ_i , and these equalities yield an incident-polarization-independent SHEL at all θ_i . We also show that a relaxed condition can yield the polarization-independent SHEL at near-normal incidence.

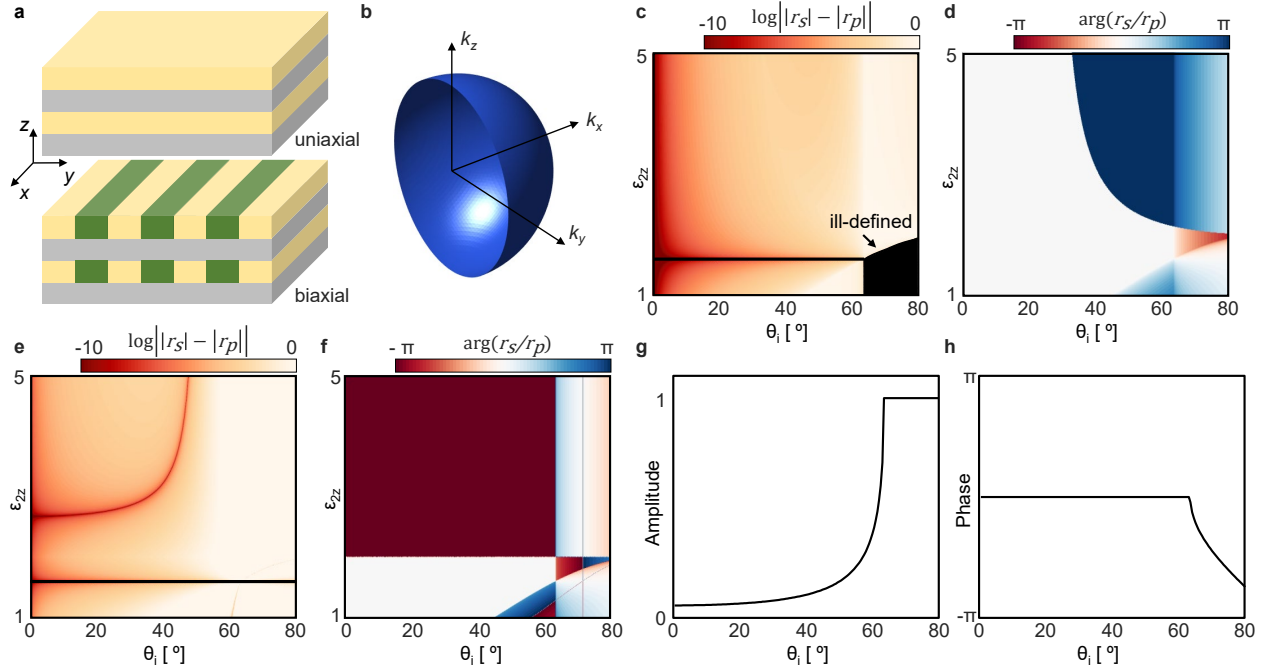


Figure 2: Optical properties of an anisotropic medium ($\varepsilon_2 = \text{diag}(\varepsilon_{2x}, \varepsilon_{2y}, \varepsilon_{2z})$). (a) Schematic of the anisotropic medium consisting of isotropic materials. (Top) Uniaxial anisotropic medium composed of two isotropic dielectrics and (bottom) biaxial anisotropic medium composed of three isotropic dielectrics. (b) A half of isofrequency contour ($k_x > 0$) of the anisotropic medium for $\varepsilon_{2x} = 2.5, \varepsilon_{2y} = \varepsilon_{2z} = 1.6$. (c) Amplitude and (d) phase difference of r_s and r_p at an interface between an isotropic dielectric ($\varepsilon_1 = 2$) and the anisotropic medium ($\varepsilon_{2x} = 2.5$ and $\varepsilon_{2y} = 1.6$) for various θ_i and ε_{2z} . The amplitude difference on a logarithmic scale is ill-defined in the black-shaded area (where $|r_s| = |r_p|$). (e) Amplitude and (f) phase difference of \dot{r}_s and \dot{r}_p at the interface. (g) Amplitude and (h) phase of r_s and r_p when $\varepsilon_{2z} = 1.6$. The two reflection coefficients are equal in the whole range and thus appear as a single curve.

Two linear polarizations, s and p , are degenerate at an interface between two isotropic media under normal incidence. Thus, the interface only supports polarization-independent reflection coefficients $r_s = -r_p$ at $\theta_i = 0^\circ$, where the minus sign is attributed to the sign convention in Fresnel equations [26]. To increase the degrees of freedom, we examine a low-symmetry case of an anisotropic medium ($\varepsilon_2 = \text{diag}(\varepsilon_{2x}, \varepsilon_{2y}, \varepsilon_{2z})$). If two of the three permittivities are the same, the medium is uniaxial and can be realized by combining two isotropic dielectric materials (Fig. 2a, top). For the most general case of $\varepsilon_{2x} \neq \varepsilon_{2y} \neq \varepsilon_{2z}$, the medium is biaxial and can be realized by stacking different isotropic dielectrics (Fig. 2a, bottom). The isofrequency contour of the medium follows

$$\frac{1}{k_0^2} \left(\frac{k_x^2 + k_y^2}{\varepsilon_{2z}} + \frac{k_x^2 + k_z^2}{\varepsilon_{2y}} + \frac{k_y^2 + k_z^2}{\varepsilon_{2x}} \right) - \left(\frac{k_x^2}{\varepsilon_{2y}\varepsilon_{2z}} + \frac{k_y^2}{\varepsilon_{2x}\varepsilon_{2z}} + \frac{k_z^2}{\varepsilon_{2x}\varepsilon_{2y}} \right) \frac{k_x^2 + k_y^2 + k_z^2}{k_0^4} = 1, \quad (9)$$

half of which ($k_x > 0$) is represented in Fig. 2b. The Fresnel coefficients at an interface between the anisotropic and isotropic (ε_1) medium can be represented as

$$\begin{aligned} r_s &= \frac{\sqrt{\varepsilon_1 - \beta^2} - \sqrt{\varepsilon_{2y} - \beta^2}}{\sqrt{\varepsilon_1 + \beta^2} + \sqrt{\varepsilon_{2y} - \beta^2}}, \\ r_p &= \frac{\sqrt{\varepsilon_1 - \beta^2}/\varepsilon_1 - \sqrt{\varepsilon_{2x} - \beta^2\varepsilon_{2x}/\varepsilon_{2z}}/\varepsilon_{2x}}{\sqrt{\varepsilon_1 - \beta^2}/\varepsilon_1 + \sqrt{\varepsilon_{2x} - \beta^2\varepsilon_{2x}/\varepsilon_{2z}}/\varepsilon_{2x}} \end{aligned} \quad (10)$$

where $\beta = \sqrt{\varepsilon_1} \sin \theta_i$ is the propagation constant. Eq. 10 shows that $r_s = r_p$ for any θ_i if

$$\varepsilon_{2x}\varepsilon_{2y} = \varepsilon_{2x}\varepsilon_{2z} = \varepsilon_1^2. \quad (11)$$

This condition does not require the use of dispersive materials and can be readily fulfilled with positive permittivities by combining several dielectric materials (Fig. 2a, see Supporting information S1).

To investigate the Fresnel coefficients for different permittivities numerically, amplitude difference on a logarithmic scale (Fig. 2c) and phase difference (Fig. 2d) of r_s and r_p when $\varepsilon_1 = 2$, $\varepsilon_{2x} = 2.5$, and $\varepsilon_{2y} = 1.6$ are obtained. Indeed, the condition $r_s = r_p$ is satisfied at all θ_i when $\varepsilon_{2z} = 1.6$, where Eq. 11 is satisfied. The equality at all θ_i automatically imposes the equality of their derivatives, $\dot{r}_s = \dot{r}_p$ (Fig. 2e and f). Amplitude and phase of r_s and r_p when $\varepsilon_{2z} = 1.6$ demonstrate clearly that the Fresnel coefficients are equal and thus the two conditions $r_s = r_p$ and $\dot{r}_s = \dot{r}_p$ are satisfied in the entire range of θ_i (Fig. 2g and h).

Furthermore, the two conditions of $r_s = r_p$ and $\dot{r}_s = \dot{r}_p$ are also satisfied under normal incidence for any ε_{2z} if $\varepsilon_{2x}\varepsilon_{2y} = \varepsilon_1^2$ is satisfied (Fig. 2c-f) for the following reasons. First, one can notice straightforwardly from Eq. 10 that ε_{2z} does not affect on r_s or r_p when $\theta_i = 0^\circ$. Thus, a medium that supports $\varepsilon_{2x}\varepsilon_{2y} = \varepsilon_1^2$ satisfies $r_s = r_p$ under normal incidence, regardless of ε_{2z} (Fig. 2c and d). Secondly, taking the first-order derivative of Eq. 10 with respect to θ_i proves that $\dot{r}_s = \dot{r}_p = 0$ for any permittivity at $\theta_i = 0^\circ$. Thus, $\dot{r}_s = \dot{r}_p$ holds automatically under normal incidence, which is also confirmed by numerical results (Fig. 2e and f). While this discussion assumes the normal incidence, in which the SHEL does not occur, both r_s/r_p and \dot{r}_s/\dot{r}_p are close to unity with extremely high accuracy at small θ_i (Fig. 2c-f, see supporting information S2). Thus, the incident-polarization-independent SHEL is expected at a sufficiently small θ_i if $\varepsilon_{2x}\varepsilon_{2z} \neq \varepsilon_{2x}\varepsilon_{2y} = \varepsilon_1^2$.

4 The polarization-independent SHEL under arbitrarily polarized incidence

To verify that the spin Hall shifts under arbitrarily polarized incidences are degenerate even when the large beam waist condition (Eq. 1) does not hold, the SHEL at the interface that satisfies Eq. 11 ($\varepsilon_1 = 2$, $\varepsilon_{2x} = 2.5$, $\varepsilon_{2y} = \varepsilon_{2z} = 1.6$, Fig. 2g and h) is considered under $N = 500$ incidences, whose polarization states are randomly distributed over the Poincaré sphere (Fig. 3). Each incidence has randomly assigned Stokes parameters (S_1, S_2, S_3) that obey $\sum_{i=1}^3 S_i^2 = 1$. In calculations, we use $w_0 = 5\lambda$ to break the large beam waist condition (Eq. 1) at small θ_i ($< 20^\circ$). In this tightly-confined regime, δ^\pm/λ calculated by the exact (Eq. 7) and approximated (Eq. 8) formulas deviate from each other (Fig. 3a and b, dashed and solid curves respectively). Whereas the polarization-dependent spin Hall shifts under these N arbitrarily polarized

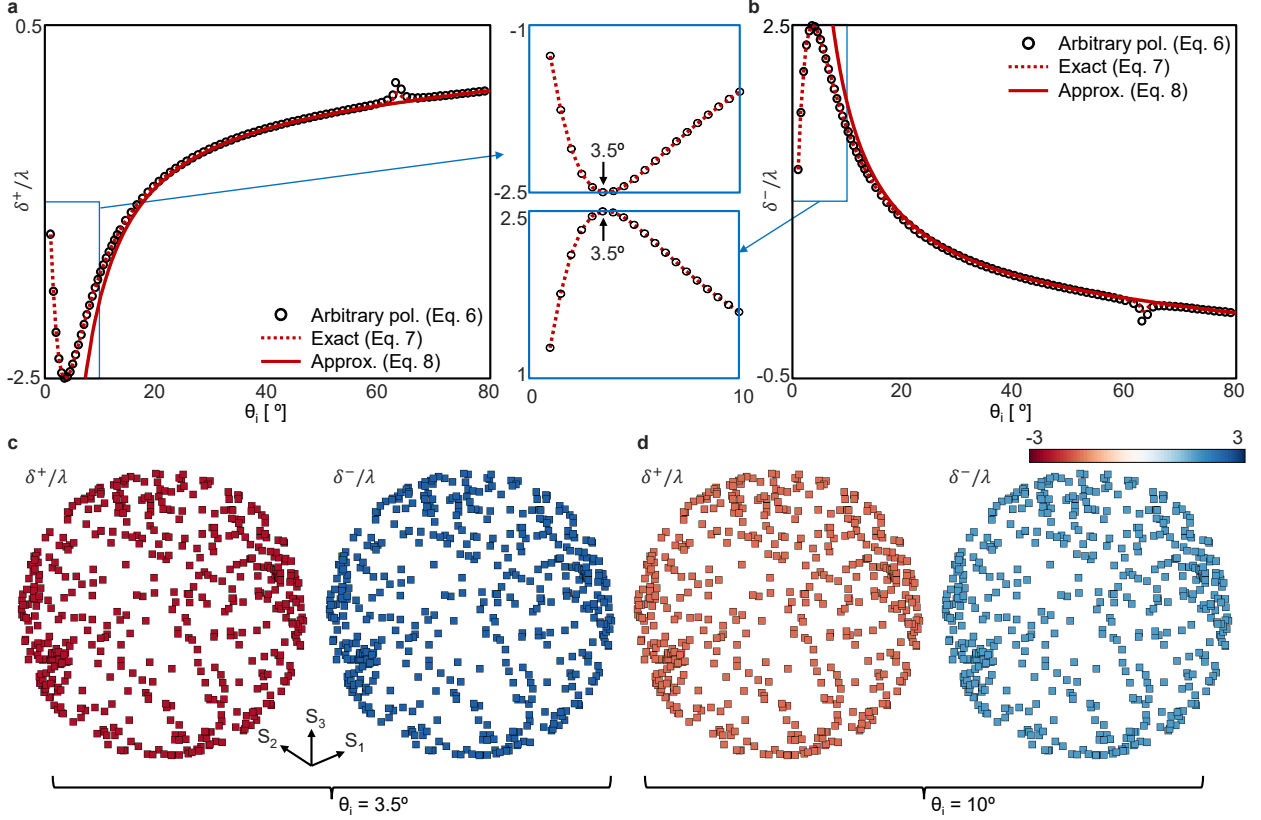


Figure 3: The spin Hall shift of N number of arbitrarily polarized incidences. (a) δ^+/λ and (b) δ^-/λ under N incidences calculated by Eq. 6. All δ/λ have the same degenerate value and appear as a single marker at each θ_i . Dashed and solid curves correspond to δ/λ obtained from the exact (Eq. 7) and approximated (Eq. 8) formulas respectively. Plots in blue boxes show a magnified view at $\theta_i \leq 10^\circ$. (c, d) δ^\pm/λ represented in Poincaré sphere when (c) $\theta_i = 3.5^\circ$ and (d) $\theta_i = 10^\circ$.

incidences have distinct values at a given θ_i and are scattered around [10] (see supporting information S2), the shifts here are independent of the incident polarization in the entire range and appear as a single marker at each θ_i . In particular, at $\theta_i = 3.5^\circ$, the polarization-independent spin Hall shift reaches $\pm w_0/2$ (Fig. 3a and b, insets), which is the maximum available value [25]. In short, a gigantic SHEL that is comparable to w_0 and reaches the theoretical upper limit occurs independent of polarization. Small peaks near $\theta_i = 60^\circ$ (Fig. 3a and b) originate from the diverging \dot{r}_s and \dot{r}_p at a critical angle (Fig. 2g and h).

For completeness, the spin Hall shifts under N incidences are represented on the Poincaré sphere for two different angles, $\theta_i = 3.5^\circ$ (Fig. 3c) and $\theta_i = 10^\circ$ (Fig. 3d). The spin Hall shifts are degenerate to the result of the exact formula (Eq. 7) regardless of the Stokes parameters of the incidence. Naturally, the standard deviation is zero at all θ_i and is not shown here. In contrast, an interface with $\varepsilon_{2x}\varepsilon_{2z} \neq \varepsilon_{2x}\varepsilon_{2y} = \varepsilon_1^2$ satisfies $r_s = r_p$ and $\dot{r}_s = \dot{r}_p$ only under normal incidence and hence yields the polarization-insensitive SHEL at a small θ_i ($< 5^\circ$, see Supporting information S2). Considering that the large SHEL appears at the small θ_i , this relaxed condition can be a promising alternative to realize polarization-independent spin Hall shift in a beam waist scale.

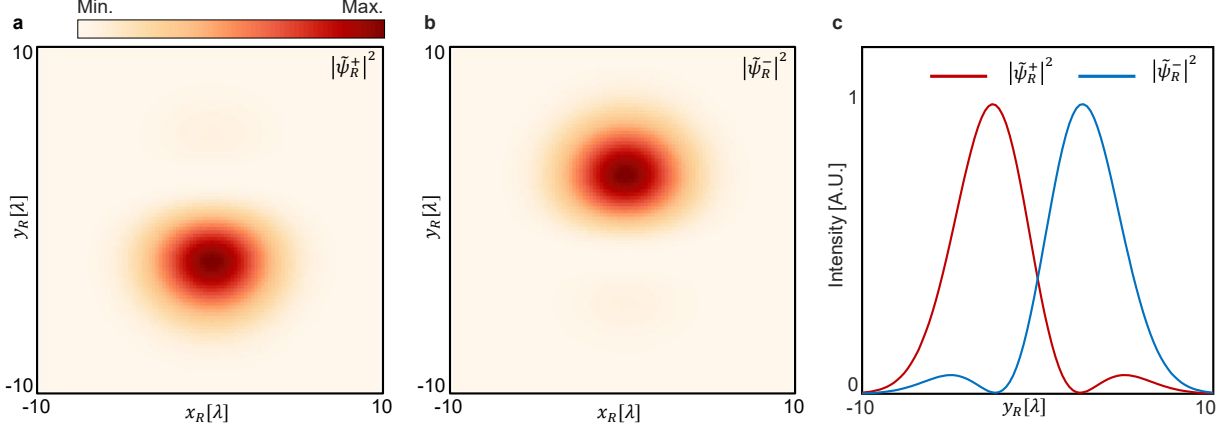


Figure 4: A discernible SHEL reaching a half beam waist under unpolarized incidence at $\theta_i = 3.5^\circ$. Intensity profiles of (a) LCP and (b) RCP components. (c) A cross-sectional view of intensities along the y_R -axis.

5 The large SHEL reaching a half beam waist and its demonstration as a beam splitter

To demonstrate the huge spin Hall shift that reaches $w_0/2$, the spatial field distributions of the circularly polarized components of the reflected beams are examined under unpolarized incidence (Fig. 4). Whereas the spin Hall shift is generally much smaller than w_0 and is not manifested visually [10, 19], here the spin Hall shift along the opposite directions of the y_R -axis is clearly distinguished (Fig. 4a and b). A cross-sectional view along the transverse axis demonstrates perceptible spin-dependent splitting (Fig. 4c). A weak side lobe centered at the opposite direction (approximately at -5λ) is observed for each LCP and RCP component. Between the side lobe and the maximum peak, the first minimum of the beam shape is located at $\pm 2.4\lambda$, which is closer to the center than the maximum of the oppositely circularly polarized beam is. Thus, according to the Rayleigh criterion, the splitting is resolvable when examined by the whole intensity. It is worth to emphasize that this large SHEL originates from the violation of the large beam waist condition (Eq. 1), and hence the beam-waist-scale, polarization-insensitive SHEL cannot be realized using the previous condition of $r_s = r_p$ only [10].

Interestingly, the spin Hall shift is degenerate under all polarization states, but the intensity ratio between the LCP and RCP components is not. Thus, this SHEL can be exploited in intensity-tunable devices by modulating the incident polarization states. To prove this point, the intensity distribution of the reflected beam is examined for five different incident polarizations (Fig. 5). Firstly, in contrast to polarization-dependent SHEL, in which the direction and magnitude of the splitting change as the incident polarization varies, incidences with different polarization states produce the same spin Hall shift (Fig. 1b-f). Meanwhile, the intensity splitting between LCP and RCP components directly follows the handedness of the incidence, i.e., its S_3 . More specifically, the intensities of the circularly polarized components are associated with the third Stokes parameter of the incidence as $\int |\psi_R^\pm|^2 d\mathbf{r} = (1 \mp S_3)/2$. Under circularly polarized incidence, the entire reflected beam undergoes a displacement without being split (Fig. 5b and f). In contrast, the reflected beam is split into two peaks with unequal intensities when the incidence is elliptically polarized (Fig. 5c and e). Under linearly polarized incidence, two equally-split peaks, each for LCP and RCP, appear. Whereas the SHEL that is much smaller than the beam waist can be resolved only through amplification, the two peaks are identifiable (Fig. 5d). The linear polarization state at the center ($y_R = 0$) is mirror-symmetric to the incident polarization with respect to the y_R -axis as a result of the π -shifted phase of r_p .

We demonstrate the polarization-independent SHEL of the tightly-confined beam where w_0 is comparable to λ as a proof-of-concept. However, it should be noted that a beam that has $w_0 \gg \lambda$ can also violate the large beam waist condition (Eq. 1) at a sufficiently small θ_i ($\ll 1^\circ$) and our theory is also applicable to this regime. In such a case, the upper limit of the spin Hall shift ($w_0/2$) becomes even greater as a result of the large w_0 , but the SHEL requires a precise setting of the ultrasmall θ_i (see supporting information S3).

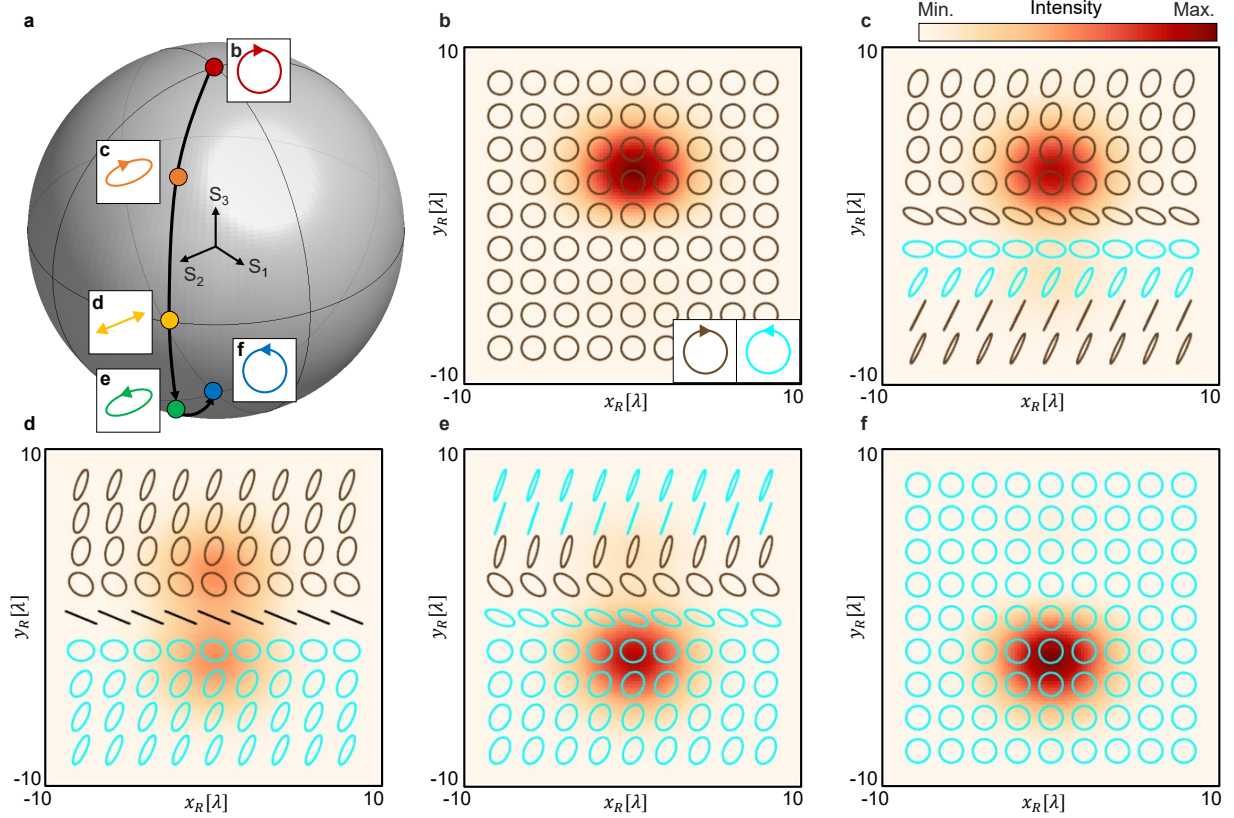


Figure 5: The SHEL as a beam splitter at $\theta_i = 3.5^\circ$. (a) Poincaré sphere with five polarization states marked. (b-f) The intensity profiles and local polarization states of the reflected beam under incidences whose polarization states are represented as (b) red, (c) orange, (d) yellow, (e) green, and (f) blue markers. Cyan and brown correspond to the left and right handedness respectively. Black denotes the linear polarization.

6 Conclusion

In conclusion, an approach towards the incident-polarization-insensitive spin Hall effect of light that exhibits a discernible splitting is presented. A theoretical proof of the required conditions, $r_s = r_p$ and $\hat{r}_s = \hat{r}_p$, is given, followed by a suggestion of an interface that supports such conditions in the entire range of incident angles. Also, a relaxed condition that yields a large and polarization-independent spin Hall effect of light at a small incident angle is presented. In addition, we demonstrate the polarization independence of the spin Hall effect of light using Monte-Carlo simulations under a huge number of arbitrarily polarized incidences. The gigantic and polarization-independent splitting that is comparable to the beam waist proves potential of our work to enable spin-dependent devices that are invariable under the change of incident polarization at any angle and active splitters that act upon incident polarization.

References

- [1] M. Onoda, S. Murakami and N. Nagaosa. Hall effect of light. *Phys. Rev. Lett.* **93**(8), 083901 (2004).
- [2] O. Hosten and P. Kwiat. Observation of the spin Hall effect of light via weak measurements. *Science* **319**(5864), 787–790 (2008).
- [3] C. Imbert. Calculation and Experimental Proof of the Transverse Shift Induced by Total Internal Reflection of a Circularly Polarized Light Beam. *Phys. Rev. D* **5**, 787–796 (1972).
- [4] F. I. Fedorov. To the theory of total reflection. *J. Opt.* **15**(1), 014002–1 (2013).
- [5] X. Ling, X. Zhou, K. Huang, Y. Liu, C.-W. Qiu, H. Luo and S. Wen. Recent advances in the spin Hall effect of light. *Rep. Prog. Phys.* **80**(6), 066401 (2017).
- [6] M. I. Dyakonov and V. Perel. Current-induced spin orientation of electrons in semiconductors. *Phys. Lett. A* **35**(6), 459–460 (1971).
- [7] M. I. Dyakonov and V. Perel. Possibility of orienting electron spins with current. *JETP Lett.* **13**, 467 (1971).
- [8] K. Y. Bliokh and A. Aiello. Goos–Hänchen and Imbert–Fedorov beam shifts: an overview. *J. Opt.* **15**(1), 014001 (2013).
- [9] K. Y. Bliokh, F. J. Rodríguez-Fortuño, F. Nori and A. V. Zayats. Spin–orbit interactions of light. *Nat. Photonics* **9**(12), 796–808 (2015).
- [10] M. Kim, D. Lee and J. Rho. Spin Hall Effect under Arbitrarily Polarized or Unpolarized Light. *Laser Photonics Rev.* **15**(7), 2100138 (2021).
- [11] H. Luo, X. Zhou, W. Shu, S. Wen and D. Fan. Enhanced and switchable spin Hall effect of light near the Brewster angle on reflection. *Phys. Rev. A* **84**, 043806 (2011).
- [12] X. Yin, Z. Ye, J. Rho, Y. Wang and X. Zhang. Photonic spin Hall effect at metasurfaces. *Science* **339**(6126), 1405–1407 (2013).
- [13] W. Zhu and W. She. Enhanced spin Hall effect of transmitted light through a thin epsilon-near-zero slab. *Opt. Lett.* **40**(13), 2961–2964 (2015).
- [14] X. Zhou and X. Ling. Enhanced Photonic Spin Hall Effect Due to Surface Plasmon Resonance. *IEEE Photon. J.* **8**(1), 1–8 (2016).
- [15] T. Tang, Y. Zhang, J. Li and L. Luo. Spin Hall Effect Enhancement of Transmitted Light Through an Anisotropic Metamaterial Slab. *IEEE Photon. J.* **9**(4), 1–10 (2017).
- [16] X. Jiang, Q. Wang, J. Guo, J. Zhang, S. Chen, X. Dai and Y. Xiang. Resonant optical tunneling-induced enhancement of the photonic spin Hall effect. *J. Phys. D: Appl. Phys.* **51**(14), 145104 (2018).
- [17] X. Jiang, J. Tang, Z. Li, Y. Liao, L. Jiang, X. Dai and Y. Xiang. Enhancement of photonic spin Hall effect via bound states in the continuum. *J. Phys. D: Appl. Phys.* **52**(4), 045401 (2018).
- [18] O. Takayama, J. Sukham, R. Malureanu, A. V. Lavrinenko and G. Puentes. Photonic spin Hall effect in hyperbolic metamaterials at visible wavelengths. *Opt. Lett.* **43**(19), 4602–4605 (2018).
- [19] M. Kim, D. Lee, T. H. Kim, Y. Yang, H. J. Park and J. Rho. Observation of enhanced optical spin Hall effect in a vertical hyperbolic metamaterial. *ACS Photonics* **6**(10), 2530–2536 (2019).
- [20] H. Dai, L. Yuan, C. Yin, Z. Cao and X. Chen. Direct Visualizing the Spin Hall Effect of Light via Ultrahigh-Order Modes. *Phys. Rev. Lett.* **124**, 053902 (2020).
- [21] M. Kim, D. Lee, B. Ko and J. Rho. Diffraction-induced enhancement of optical spin Hall effect in a dielectric grating. *APL Photonics* **5**(6), 066106 (2020).

- [22] M. Kim, D. Lee, H. Cho, B. Min and J. Rho. Spin Hall Effect of Light with Near-Unity Efficiency in the Microwave. *Laser Photonics Rev.* **15**(2), 2000393 (2021).
- [23] Y. Yang, T. Lee, M. Kim, C. Jung, T. Badloe, D. Lee, S. Lee, H.-J. Lee and J. Rho. Dynamic optical spin Hall effect in chitosan-coated all-dielectric metamaterials for a biosensing platform. *IEEE J. Sel. Top. Quantum Electron.* (2021).
- [24] M. Kim, D. Lee, T. H.-Y. Nguyen, H.-J. Lee, G. Byun and J. Rho. Total Reflection-Induced Efficiency Enhancement of the Spin Hall Effect of Light. *ACS Photonics* (2021).
- [25] C. Miao, D. Wang, E. Herrmann, Z. Zheng, H. Huang and H. Gao. *Sci. Rep.* (To be published (<https://www.researchsquare.com/article/rs-723490/v1>)).
- [26] M. Born and E. Wolf. Principles of optics: electromagnetic theory of propagation, interference and diffraction of light. Cambridge University Press (2013).